

3-D parameter-space electromagnetic mapping using helicopter-borne systems

Haoping Huang* and Douglas C. Fraser
 Geotrex-Digheem, a division of CGG Canada Ltd.

Summary

Interpretation of helicopter-borne EM data is commonly based on the mapping of resistivity (or conductivity) under the assumption that the magnetic permeability and dielectric permittivity are the same as those of free space (Fraser, 1978). This is actually 1-D parameter-space EM mapping to a half-space model. The EM data obtained from a multi-frequency EM system may contain information about the magnetic permeability and dielectric permittivity as well as the conductivity. Prior work (Huang and Fraser, 1998; Huang et al, 1998) has shown how 2-D parameter-space EM mapping may be performed with resistivity and magnetic permeability and with resistivity and dielectric permittivity. An algorithm has now been developed to perform 3-D parameter-space EM mapping based on a half-space model with variable resistivity, magnetic permeability and dielectric permittivity. A field example shows that the algorithm for 3-D parameter-space EM mapping yields better results than 2-D parameter-space mapping when the survey area exhibits both permeable and dielectric properties.

Introduction

Interpretation of helicopter EM mapping data is commonly based on the computation of resistivity under the assumption that the magnetic permeability and dielectric permittivity are the same as those of free space (Fraser, 1978). As shown in Figure 1a, this is 1-D parameter-space EM mapping along the σ -axis. However, EM data obtained from a multifrequency EM system contains information about the magnetic permeability and dielectric permittivity as well as the conductivity ($=1/\text{resistivity}$). As the frequency range of helicopter-borne EM systems increases and the noise level decreases, it is possible to transform the EM data from different frequencies to these three physical parameters.

Huang and Fraser (1998) developed a resistivity and magnetic permeability mapping technique under the assumption that the earth is a magnetic conductive half-space with a dielectric permittivity of free space. This is 2-D parameter-space EM mapping in the σ - μ_r plane. Huang et al (1998) developed a resistivity and dielectric permittivity mapping technique under the assumption that the earth is a lossy conductive homogeneous half-space with a magnetic permeability of free space. This is 2-D parameter-space EM mapping in the ϵ_r - σ plane. Since the resistivity or conductivity of the earth always affects the

EM data in the frequency range used in helicopter EM systems, no attempt has been made to perform 2-D mapping in the ϵ_r - μ_r plane.

The effect of dielectric permittivity on the EM data is similar to that of magnetic permeability in that both tend to decrease the inphase and increase the quadrature response. In resistive areas, the magnetic and dielectric effects will both be present in high frequency EM data while only the magnetic effect will exist in low frequency data. When 2-D parameter-space EM mapping in the ϵ_r - σ plane is performed, the dielectric permittivity and resistivity computed from the high frequency will both be erroneously high due to the magnetic effect. Therefore, it is necessary to consider 3-D parameter-space mapping to avoid this problem. This paper is concerned with the mapping of any point p in the 3-D parameter space ϵ_r - σ - μ_r , using multifrequency helicopter EM data. The model used in this study is a half-space with variable conductivity, magnetic permeability and dielectric permittivity.

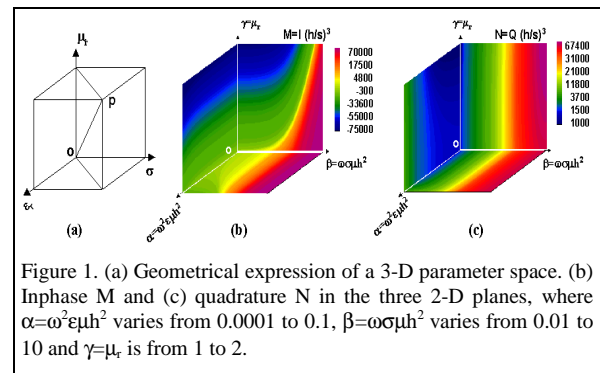


Figure 1. (a) Geometrical expression of a 3-D parameter space. (b) Inphase M and (c) quadrature N in the three 2-D planes, where $\alpha = \omega^2 \epsilon_r \mu_r^2$ varies from 0.0001 to 0.1, $\beta = \omega \sigma \mu_r^2$ varies from 0.01 to 10 and $\gamma = \mu_r$ is from 1 to 2.

Theory and method

The effects of conduction, magnetization and dielectric polarization on the EM data can be found from the forward modeling of half-spaces. For closely coupled transmitting and receiving coils, as exists in frequency domain helicopter EM systems, the ratio of secondary magnetic field intensity H_s to primary magnetic field intensity H_o , at the receiving coil, can be approximated as (Fraser, 1972),

$$H_s/H_o = (s/h)^3 [M(\theta, \mu_r) + iN(\theta, \mu_r)], \quad (1)$$

where h is the EM sensor height above the earth, s is the coil separation, and $\theta = (-\omega^2 \epsilon_r \mu_r^2 + i \omega \sigma \mu_r^2)^{1/2}$ is the induction

3-D parameter-space EM mapping

number. ω is the angular frequency, σ is conductivity, μ is the magnetic permeability and ϵ is the dielectric permittivity. In applied geophysics, we often deal with resistivity $\rho=1/\sigma$, relative magnetic permeability $\mu_r = \mu/\mu_0$ and relative dielectric permittivity (dielectric constant) $\epsilon_r = \epsilon/\epsilon_0$, where μ_0 and ϵ_0 are the magnetic permeability and dielectric permittivity of free space, respectively. The measured inphase I and quadrature Q amplitudes may be represented as

$$I = (s/h)^3 M \text{ and } Q = (s/h)^3 N \quad (2)$$

where the I and Q amplitudes are expressed in units of parts per million (ppm) of the primary magnetic field intensity H_0 at the receiving coil.

M and N respectively are the inphase and quadrature components of the response function $M+iN$, which themselves are functions of θ and μ_r . Equations (1) and (2) are valid on the assumption that $s^3 \ll h^3$. This *superimposed dipole assumption* (Grant and West, 1965) is generally valid for surveys flown with all commercial helicopter EM systems.

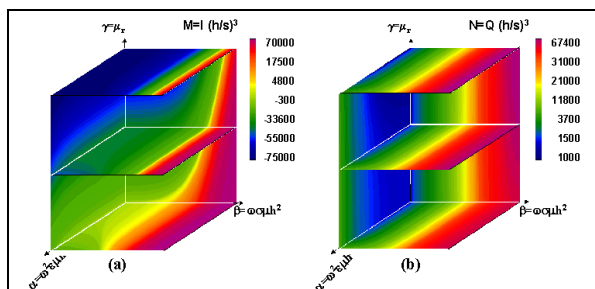


Figure 2. The inphase M (a) and quadrature N (b) as a function of α , β and γ , where $\alpha=\omega^2\epsilon_r h^2$ and $\beta = \omega\sigma h^2$ increase continually along their axes and $\gamma, =\mu_r$ increases discretely.

Figure 1a is a simplified picture of 3-D parameter mapping. We actually employ the horizontal axes of α , β (e.g., Figure 1b) rather than ϵ_r , σ where α and β are derived from the real and imaginary components of the squared induction number $\theta^2 = -\omega^2\epsilon_r h^2 + i\omega\sigma h^2$.

It is interesting to view the gross behavior of the inphase M and quadrature N components as conductivity, magnetic permeability and dielectric permittivity vary. For example:

- 1) For the β - γ plane, we see that magnetic permeability and conductivity are roughly equal in their impact on the inphase M component since the colors trend roughly 45 degrees to the axes (Figure 1b). However, magnetic permeability has little impact on the quadrature N component, which is governed primarily by the conductivity, since the colors trend parallel to the γ axis.

- 2) For the α - β plane, we see that the dielectric permittivity has a small impact on the inphase M (Figure 1a) and very little impact on the quadrature N (Figure 1b). The conductivity has a major impact on both the inphase and quadrature components.
- 3) For the α - γ plane, we see that the dielectric permittivity has a lesser impact on the inphase M than does the magnetic permeability (Figure 1b), whereas the reverse is true for the quadrature N (Figure 1c).

It is the interaction of the three parameters which is important. All must be dealt with in the transformation of the measured EM responses to allow the correct recovery of the electric properties of a dielectric magnetic earth.

We may use other presentations to show the inphase and quadrature components in 3-D parameter space. For example, Figure 2 presents the (a) inphase M and (b) quadrature N as a function of α and β and for three slices through the γ ($=\mu_r$) axis. Each such presentation provides insight into the behavior of the EM response to the three earth parameters.

Table 1. Inphase I and quadrature Q in ppms for 1-D, 2-D and 3-D parameter space. The four models have a resistivity of 10,000 ohm-m and have variable magnetic permeability and dielectric permittivity.

f	Model 1 $\mu_r=1 \ \epsilon_r=1$		Model 2 $\mu_r=1.02 \ \epsilon_r=1$		Model 3 $\mu_r=1 \ \epsilon_r=8$		Model 4 $\mu_r=1.02 \ \epsilon_r=8$	
	I	Q	I	Q	I	Q	I	Q
105k	33.1	117.6	-8.0	119.7	-4.1	136.9	-45.8	139.3
25k	4.7	32.1	-36.5	32.7	1.9	32.8	-39.4	33.4
6200	0.7	8.7	-40.6	8.9	0.5	8.7	-40.8	8.9
1600	0.1	2.4	-41.3	2.4	0.1	2.4	-41.3	2.4
385	0.0	0.6	-41.4	0.6	0.0	0.6	-41.4	0.6

While the above figures show the gross behavior of the EM, it may help our understanding to view the behavior in detail. Table 1 shows the inphase and quadrature responses for four half-space models. The frequencies shown are from a new DIGHEM resistivity mapping system with all horizontal coplanar coils. We consider here only the impact of magnetic permeability and dielectric permittivity on the 105k Hz data of table 1.

Compare model 2 ($\mu_r=1.02$, $\epsilon_r=1$) with model 1 ($\mu_r=\epsilon_r=1$): we see that the magnetic permeability causes the inphase I to decrease from 33 ppm to -8 ppm. Compare model 3 ($\mu_r=1$, $\epsilon_r=8$) with model 1 ($\mu_r=\epsilon_r=1$): we see that the dielectric permittivity causes the inphase to decrease from 33 ppm to -4 ppm. Model 4 encompasses both the magnetic permeability of model 2 and the dielectric permittivity of model 3. We see that the combined magnetic permeability and dielectric permittivity has had a much stronger impact

3-D parameter-space EM mapping

on the inphase, causing it to decrease from 33 ppm to -46 ppm.

This example shows that 3-D parameter-space EM mapping is necessary in areas where the ground is magnetically and dielectrically polarizable. The transformation algorithm, described below, correctly returns the three earth parameters when the earth is homogeneous.

The EM data obtained from the lowest DIGHEM frequency, usually 385 Hz or 900 Hz, is free of dielectric effect because the ratio of displacement current to conduction current tends to zero as $\omega\epsilon/\sigma \rightarrow 0$. Therefore, the relative magnetic permeability can be obtained from the inphase and quadrature response at the lowest frequency (Huang and Fraser, 1998). The computed magnetic permeability is then used along with the inphase and quadrature response at the highest frequency to obtain the relative dielectric permittivity. The apparent resistivity can be computed using either the homogeneous half-space or the pseudo-layer half-space model (Fraser, 1978).

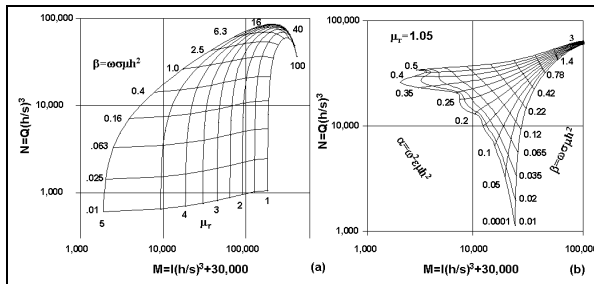


Figure 3. (a) The phasor diagram of the inphase M and quadrature N response functions for the half-space model of a magnetic conductive earth for several values of $\beta = \omega\sigma\mu h^2$ and relative permeabilities μ_r . (b) The phasor diagram of the inphase M and quadrature N for the half-space model of a dielectric conductive earth for several values of $\alpha = \omega^2\epsilon\mu h^2$ and $\beta = \omega\sigma\mu h^2$ and a relative permeability μ_r of 1.05.

Figure 3 shows the phasor diagrams of the inphase M and quadrature N response functions for a homogeneous half-space model with variable resistivity, magnetic permeability and dielectric permittivity. The phasor diagram in Figure 3(a) was constructed by taking the inphase I and quadrature Q ppms from the forward solutions of many half spaces, followed by a transformation of the ppms to the normalized inphase M and quadrature N components using equation (2). In order to plot the diagram in logarithmic space, M' is taken as M with 30,000 added to ensure that this quantity remains positive. The inputs to the phasor diagram or the equivalent algorithm are therefore the normalized inphase M and quadrature N components. The outputs from the algorithm are $\beta = \omega\sigma\mu h^2$ and μ_r and

then the resistivity ρ can be obtained from β under the assumption that the bird altitude from the altimeter can be used in place of the unknown sensor-source height. The β value serves also as an indication of the resolvability of the relative permeability μ_r . If β is low, the value of μ_r from Figure 3a is likely to be reliable. If β is greater than 6, the relative permeability μ_r will not be reliable.

Figure 3b was constructed in a similar manner to that of Figure 3a. Figure 3b can be used to obtain the dielectric permittivity and resistivity from the inphase and quadrature data at the highest frequency given the relative permeability μ_r . Figure 3b is derived from a 3-D image with axes M , N and μ_r . For simplicity, only the slice for $\mu_r = 1.05$ is displayed.

If the earth is a true homogeneous half-space, the relative magnetic permeability μ_r and relative permittivity ϵ_r obtained from Figure 3 would be the true relative values. Otherwise, they would be the apparent values.

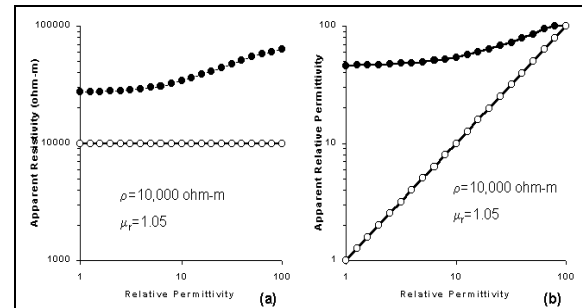


Figure 4. The (a) apparent resistivity and (b) apparent permittivity are shown for a homogeneous half-space model having a resistivity of 10,000 ohm-m, a relative permeability of 1.05, and a relative dielectric permittivity which increases from left to right. The curves with solid circles are from 2-D α - β plane mapping, and those with open circles are from 3-D α - β - γ parameter-space mapping. The frequency used is 56k Hz

Figure 4 is a synthetic example showing the importance of 3-D parameter mapping when the magnetic permeability and the dielectric permittivity are greater than those of free space. The model is a homogeneous half-space with a resistivity of 10,000 ohm-m and a relative permeability of 1.05. The relative dielectric permittivity increases from left to right from 1 to 100. Figure 4a shows that the apparent resistivity (solid circles) computed from 56k Hz EM data is significantly overestimated in α - β plane mapping where magnetic permeability is ignored. When the magnetic permeability obtained from the lowest frequency is used as an input to the 3-D mapping algorithm, the true resistivity is obtained (open circles).

In the case of dielectric permittivity, Figure 4b shows that the computed apparent permittivity is also significantly

3-D parameter-space EM mapping

overestimated in $\alpha\beta$ plane mapping. In particular, when the dielectric permittivity of the ground is low, a false dielectric high could be generated due to the ignored magnetic permeability. When the magnetic permeability obtained from the lowest frequency is used as an input to the 3-D mapping algorithm, the true dielectric permittivity is obtained (open circles).

A field example

Figure 5 is a field example from Northern Canada showing the cross-coupling of the computed electrical properties when a parameter is ignored. The highest and lowest frequencies of the DIGHEM system used in this survey are 56k Hz and 900 Hz, respectively. The apparent magnetic permeability is derived from the lowest frequency data and then converted to the apparent susceptibility as shown in Figure 5b. The similarity with the magnetometer map of Figure 5a is to be expected since the geology is steeply dipping and the overburden is thin. Both the EM and the magnetometer are virtually sampling the same geology even though the depth of exploration of the magnetometer is much greater than that of the helicopter EM system.

Figures 5c and 5d respectively show the apparent resistivity and apparent permittivity map computed from EM data at 56k Hz using the 2-D ($\alpha\beta$) mapping method, i.e., permeability is ignored. As can be seen, some of the magnetic features, as indicated by dike and fault patterns, appear on the resistivity and dielectric permittivity maps. The magnetic rocks cause the computed resistivity and permittivity to be too high since the inphase is decreased by magnetic polarization. Figures 5e and 5f are the apparent resistivity and apparent permittivity map derived from EM data at 56k Hz, with the computed magnetic permeability as input, i.e. using the 3-D ($\alpha\beta\gamma$) mapping method. The magnetic features do not appear on the maps of resistivity and permittivity.

Conclusions

New methods for 3-D parameter-space mapping have been developed for helicopter-borne electromagnetic systems. The model used in this study is a half-space with variable resistivity, magnetic permeability and dielectric permittivity. Since the EM data obtained from the lowest DIGHEM frequency is free of dielectric effect, the relative magnetic permeability can be obtained from the inphase and quadrature at the lowest frequency. The computed magnetic permeability is then used along with the inphase and quadrature at the highest frequency to obtain the relative dielectric permittivity. The resistivity may be computed for each frequency, using the magnetic permeability and dielectric permittivity as input if required. This procedure avoids errors in the computed dielectric permittivity caused by the magnetic effect, and it avoids

errors in the computed resistivity from both magnetic and dielectric effects. A field example shows that magnetic rocks could produce false features on the resistivity and dielectric permittivity maps when magnetic permeability is ignored. Conversely, the maps derived from 3-D parameter-space EM mapping are free of such artifacts.

References

- Fraser, D. C., 1972, A new multicoil aerial electromagnetic prospecting system: *Geophysics*, **27**, 518-537.
- Fraser, D. C., 1978, Resistivity mapping with an airborne multicoil electromagnetic system: *Geophysics*, **43**, 144-172.
- Grant, F. S. and West, G. F., 1965, *Interpretation theory in applied geophysics*: McGraw-Hill.
- Huang, H., and Fraser, D.C., 1998, Magnetic permeability and electric resistivity mapping with a multifrequency airborne EM system: *Exploration Geophysics*, **29**, 249-253.
- Huang, H., Hodges, G., and Fraser, D. C., 1998, Mapping dielectric permittivity and resistivity using high frequency helicopter-borne EM data: 68th Ann. Internat. Mtg., Soc. Expl. Geophys., Expanded Abstracts, 817-82.

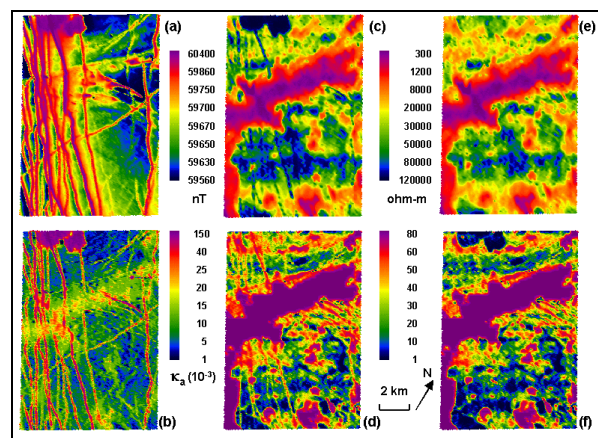


Figure 5. (a) The magnetic total field. (b) The apparent magnetic susceptibility obtained from the inphase and quadrature amplitudes at 900 Hz. (c) The apparent resistivity and (d) the apparent permittivity obtained from the inphase and quadrature at 56k Hz ($\alpha\beta$ plane 2-D mapping). (e) The apparent resistivity and (f) the apparent permittivity computed from the inphase and quadrature at 56k Hz along with the magnetic permeability ($\alpha\beta\gamma$ space 3-D mapping).